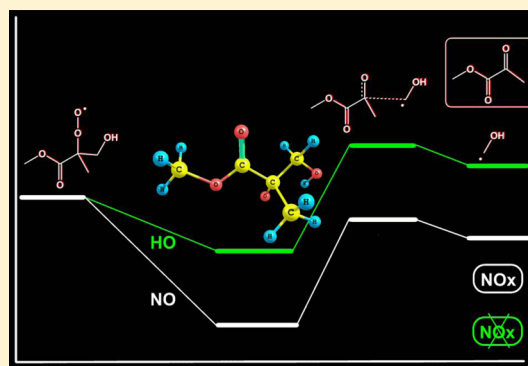


Atmospheric Degradation of $\text{CH}_2=\text{C}(\text{CH}_3)\text{C}(\text{O})\text{OCH}_3$ Initiated by OH Radicals: Mechanistic Study and Quantification of $\text{CH}_3\text{C}(\text{O})\text{C}(\text{O})\text{OCH}_3$ in NO_x Free AirRodrigo G. Gibilisco,[†] Jorge G. Uranga,[‡] Ana N. Santiago,[‡] and Mariano A. Teruel^{*,†}[†]Dpto. de Físicoquímica, Facultad de Ciencias Químicas and [‡]Dpto. de Química Orgánica, Facultad de Ciencias Químicas, Universidad Nacional de Córdoba, Instituto de Investigaciones en Físicoquímica de Córdoba (INFIQC), Ciudad Universitaria, 5000 Córdoba, Argentina

Supporting Information

ABSTRACT: The product distribution of the gas-phase reaction of OH radicals with methyl methacrylate ($\text{CH}_2=\text{C}(\text{CH}_3)\text{C}(\text{O})\text{OCH}_3$, MMA) in the absence of NO_x was studied at 298 K and atmospheric pressure of air. The experiments were performed in a Teflon chamber using solid-phase microextraction (SPME) with GC–MS and GC–FID for product identification and quantification, respectively. In the absence of NO_x , methyl pyruvate ($\text{CH}_3\text{C}(\text{O})\text{C}(\text{O})\text{OCH}_3$) was identified with a yield of $76 \pm 13\%$ in accordance with the decomposition of the 1,2-hydroxyalkoxy radicals formed. In addition, a detailed quantum chemical study of the degradation of MMA was performed by density functional theory (DFT) methods using the MPWB1K functional. This calculation suggests that formation of methyl pyruvate, from C1–C2 scission of 1,2-hydroxyalkoxy radical, is kinetically and thermodynamically the most favorable reaction path taking into account the electronic properties of reaction intermediates and transition states. The difference observed on the degradation mechanism of MMA in the presence and absence of NO_x was explained in terms of the associated thermochemistry. Furthermore, this study propose that reaction between peroxy radical (RO_2^*) and hydroxyl radical (OH) became relevant at NO_x -free environments. This statement is in agreement with recent studies concerning small peroxy radicals such as CH_3OO^* .



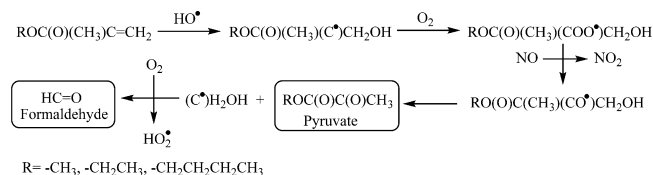
1. INTRODUCTION

Polymeric materials constructed from methyl methacrylate monomers are used in large amounts by a variety of industries due to their wide domestic and industrial uses. According to a survey conducted by the U.S. Environmental Protection Agency (EPA), the principal uses of methyl methacrylate (MMA) are cast sheet and other grades like advertising signs and displays, lighting fixtures, building panels and sidings, and coatings (latex paints, lacquer, and enamel resins).¹ Recent studies revealed that an optimized system for recycling methyl methacrylate waste is still required because it produces more than twice the amount of Greenhouse Gas (GHG) emissions than other commodity resins.²

Once in the atmosphere, MMA and similar compounds are subject to chemical degradation mainly initiated by OH radicals and, to a lesser extent, NO_3 radicals, ozone and, in certain environments, also Cl atoms.³ Kinetic studies over the OH radical reaction with MMA were performed by different techniques over the last years,^{4–7} showing that the main tropospheric removal processes of this ester proceed via OH radical initiated oxidation. However, because the rate coefficient of Cl atom reaction with MMA is nearly an order of magnitude greater than that of reaction with OH, degradation by Cl atom

could be important in the marine boundary layer and in some industrial areas as well.^{8,9}

Even though several studies were conducted on the kinetics of these compounds, research is still needed into products formed by oxidation of MMA initiated by OH radicals in different atmospheric scenarios. Previous studies described qualitatively the degradation products for a series of esters.⁴ The authors showed that alkyl pyruvates were found to be the main degradation products according to the addition of OH radicals to the less substituted carbon atom of the double bond, followed by decomposition of 1–2-hydroxyalkoxy radicals formed in the presence of NO_x through the mechanism suggested below:



Received: May 4, 2015

Revised: July 25, 2015

Published: July 27, 2015

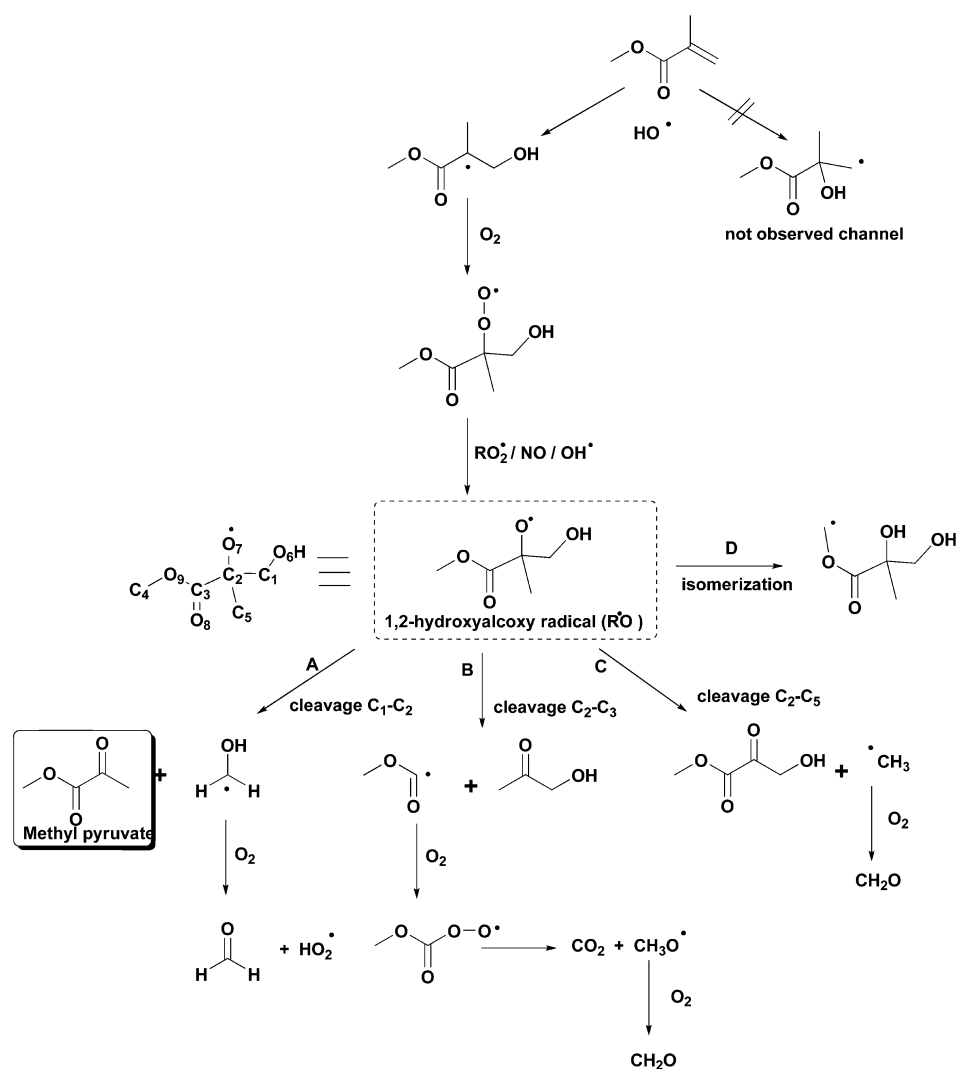


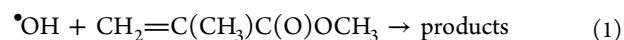
Figure 1. Simplified reaction mechanism for the addition channel in the OH radical-initiated oxidation of methyl methacrylate. The dashed line reflects the key intermediate alkoxy radical (RO^*). Inside the box, the degradation product is identified and quantified.

Gas chromatography–mass spectrometry (GC/MS) identification profiles corroborated the presence of methyl pyruvate, ethyl pyruvate, *n*-butyl pyruvate, and *n*-butyl glyoxylate as unique reaction products of methyl methacrylate, ethyl methacrylate, *n*-butyl methacrylate, and *n*-butyl acrylate, respectively, in the OH radical initiated degradation.

Recently, a quantitative study over the degradation products of methyl methacrylate in the OH radical oxidation in polluted atmospheres was performed. $\text{CH}_3\text{C}(\text{O})\text{C}(\text{O})\text{OCH}_3$, HCHO, and CO were identified as reaction products. Through the study of the time–concentration profiles of methyl pyruvate and HCHO, it was assumed that both were produced as primary products, whereas CO was reported to be formed as a secondary product. Concentrations of methyl pyruvate and HCHO gave molar yields of $92 \pm 16\%$ and $87 \pm 12\%$, respectively. These results suggest that, in the presence of NO, the decomposition channel occurs almost exclusively. In their residual FTIR product spectra, unidentified absorption bands observed in the range of 940 to 3000 were assigned to the presence of other carbonyl-containing products. Nevertheless, on the basis of the yields of methyl pyruvate and HCHO, the molar yield of these compounds was estimated to be $<8\%$.¹⁰

One of the objectives of this work was to determine the product yield of the title reaction in the absence of NO_x and atmospheric conditions so as to simulate remote or rural areas. In addition, it aimed at comparing the degradation of MMA in mechanisms and yields of reaction pathways, if any, with the chemistry of polluted areas, with large amounts of NO_x . The question arises from the evidence that the product branching ratios for the reactions of OH radicals with acrylate esters are particularly NO_x -sensitive,^{10–12} affecting the nature of reaction intermediates by promoting molecular channels as reaction with oxygen or isomerization.

The main reaction pathway for OH radical with MMA is the addition, to the double bond, of the alkene unit in the ester eq 1.



After addition of the OH radical it is well established that the subsequent chemistry will result in the formation of peroxy radicals.

Figure 1 suggests possible pathways for the reaction of methyl methacrylate with OH radicals. The main reaction pathway involves initial addition of OH radical to the terminal carbon atom of the $\text{C}=\text{C}$ bond, forming 1,2-hydroxyalkyl radicals, as seen in the mechanism proposed. The addition mechanism is

expected to account for over 98% of the reaction, predicted by the structure–reactivity relationship (SAR) calculations using the Environmental Protection Agency's rate constant calculation software, AOPWIN v1.91.¹³

The hydroxyalkyl radicals formed will react with O₂ to form the corresponding 1,2-hydroxyalkyl peroxy radicals (RO₂[•]). The peroxy radicals will then react further with several unpaired spin species to form hydroxyalkoxy radicals.

The 1,2-hydroxyalkoxy can decompose by various channels (Figure 1), which include (A) C₁–C₂ scission to give methyl pyruvate and CH₂OH radicals, (B) C₂–C₃ scission to give hydroxyacetone and CH₃OC(O) radicals, or (C) ejection of a methyl group to form methyl-3-hydroxy-2-oxopropanoate CH₂(OH)–C(O)–C(O)OCH₃. In addition to decomposition channels, the possible isomerization reaction by a 1,5-H shift (channel D) cannot be excluded; thus, it is also considered in the present analysis.

In the presence and absence of NO_x, it is well-known that peroxy radicals formed result in alkoxy radicals. It is at this phase where ongoing discussion centers on the species that lead to the formation of alkoxy radicals.¹⁴

At low NO_x concentrations, as in the remote marine and continental boundary layer, the lifetimes of RO₂[•] radicals increase and other reaction pathways become competitive for peroxy radicals. Atmospheric chemistry models consider that the major fate for RO₂[•] under these conditions is the self-reaction and cross-reactions with other RO₂ radicals or with HO₂ radicals. However, recent evidence suggests the importance of considering the reactions between OH radicals and peroxy radicals, proposing that they can become a major sink for CH₃O₂ radicals under remote conditions.^{15,16}

The above-mentioned discussion focuses on small molecules such as methyl peroxy radicals; yet, larger peroxy radicals still remain unstudied. For this reason, an exhaustive study including a theoretical analysis becomes necessary to fully understand the chemistry of these relevant atmospheric radicals.

From a computational point of view, Gao and co-workers¹⁷ recently calculated the overall rate constants of the possible channels of atmospheric oxidation of MMA toward OH and NO₃ radicals. This study described theoretically the oxidation of MMA under NO_x-rich conditions at the B3LYP/6-31G(d,p) level. The rate constants were deduced by the canonical variational transition-state (CVT) theory with the small-curvature tunneling (SCT) correction and the multichannel Rice–Ramsperger–Kassel–Marcus (RRKM) theory. Although they report a global analysis in reasonable agreement with experimental kinetic measurement, the work does not provide an exhaustive description concerning the mechanism and intermediates involved, and there is no molecular interpretation about the reactivity of these species in terms of their electronic properties.

In this work a computational study using density functional theory is presented to describe the main degradation pathways at electronic level, in view of the absence of theoretical calculations that could help gain new physical insights into the mechanism of the oxidation reaction of MMA in different environments. The conjunction of theoretical and experimental methods provides a powerful tool for a better understanding of the reaction pathways, kinetics, thermochemistry, and reactivity of atmospheric related gas-phase reactions. The results obtained allow advancing an interpretation to explain the chemistry of remotes areas. In this sense in this work we performed the first product distribution study on the reaction of MMA with OH radicals in

the absence of NO_x and the first quantitative quantum mechanistic description of the fate of the 1–2-hydroxyalkoxy radicals formed.

2. EXPERIMENTAL SECTION

The experimental setup consisted of an 80 L Teflon bag located in a wooden box with the internal walls covered with aluminum foil, and operated at atmospheric pressure 760 ± 10 Torr and 298 ± 2 K. The amounts of the organic reactants measured were flushed into the bag with a stream of synthetic air. The bag was then filled with air to its full capacity at atmospheric pressure using electronic MKS mass flow controllers (MKS 179 A, 1259 C). H₂O₂ was used to generate OH radicals by photolysis using a set of germicidal lamps eq 2.



These lamps provide UV radiation with a λ maximum around 254 nm. In the present work, six of these lamps were used to produce OH radicals. The sample was taken from the reactor after periods of 30 s photolysis. The total time of photolysis was between 2 and 5 min.

Reaction mixtures consisting of an internal standard compound and the sample organic reactant, diluted in air, were introduced in the reaction chamber and left to mix, prior to photolysis, for approximately 1 h. Before each set of experiments, the bag was cleaned by filling it with a mixture of O₂ and N₂ and photolyzed for 15–25 min using four germicidal lamps (Philips 30 W) with a UV emission at 254 nm to produce O₃. After this procedure, the bag was cleaned again by repeated flushing with air and the absence of impurities was checked by GC before performing the experiments.

Gas samples were periodically removed from the Teflon bag using the SMPE technique, DVB/CAR/PDMS coated fiber was employed because it shows good response for these compounds. The adsorption time was 15 min at 298 K and desorption was carried out into the injector port for 2 min at 473 K.

Quantification of the reaction product was performed using the internal standard technique. The internal standard compound used was acetic acid, because it showed negligible conversions at the reaction times employed. Furthermore, to eliminate possible contributions of dark reactions, mixtures of hydrogen peroxide and air with MMA and the internal standard compound were prepared and allowed to stand in the dark for 2 h. In all cases, the reaction of the organic species with the precursor of OH radicals (hydrogen peroxide), in the absence of UV light, was of negligible importance over the typical time periods used in this work.

In addition, to test for possible photolysis of the reactants, mixtures of the unsaturated ester and internal standard in air, in the absence of hydrogen peroxide, were irradiated for 30 min using the output of all the germicidal lamps surrounding the chamber. No significant photolysis of any of the reactants was observed; chromatographic areas were reproducible over time, resulting in a less than 2% variation between experiments.

The initial concentrations used in the experiments were 80–120 ppm for MMA and 50 ppm for acetic acid (1 ppm = 2.46 × 10¹³ molecules cm⁻³ at 298 K and 760 Torr of total pressure).

The organics were monitored by gas chromatography–flame ionization detector (GC–FID) (Shimadzu GC-14B), using a HP-20 M capillary column (Carbowax 20M, 25 m × 0.2 mm × 0.1 μm) held from 40 to 120 °C. The analytical technique employed for the qualitative identification of the products

formed after irradiation was GC–MS on a Shimadzu GC/MS QP 5050 gas chromatography equipped with a 30 m × 0.12 mm DB-5 MS column.

3. CALCULATION METHODS

Quantum mechanical calculations were performed with the Gaussian 09 suite of programs.¹⁸ Geometry optimization of the reactants, products, and transition states was made at the MPWB1K¹⁹ level of theory using 6-31+G(d,p) basis set because the same basis set was used for developing the model functional. This method was successfully applied to kinetic, mechanistic, and thermochemical studies over reactions with fluorinated esters^{20,21} and other carbonyl compounds.²² To determine whether the identified transition states effectively connect between reactant and products, intrinsic reaction coordinate (IRC) calculations^{23,24} were performed at the same level. The energies of relevant stationary point were refined by calculation at MPWB1K/6-311++G(d,p)//MPWB1K/6-311+G(d,p) level for comparative purposes. In all cases, spin contamination was not significant for the calculated radicals because $\langle S \rangle^2$ was found to be 0.76 at MPWB1K/6-31+G(d,p) before annihilation, only slightly larger than the expected value of $\langle S \rangle^2 = 0.75$ for doublets. The energies emerging in this paper include the unscaled ZPE corrections unless otherwise specified.

4. MATERIALS

The following chemicals with purities as stated by the supplier were used without further purification: synthetic air (Air Liquide, 99.999%), methyl methacrylate (Aldrich, 99.99%), acetic acid (Aldrich, 97%), methyl Pyruvate (Aldrich, 98%), and H₂O₂ (Cicarelli, 60 wt %).

5. RESULTS AND DISCUSSION

Product determination was performed after irradiation of H₂O₂/ester/acetic acid/air for periods of 30 s every 30 min. Photolysis of MMA in the absence of radical precursor, dark reactions, and wall losses were negligible compared with the loss in the OH radical initiated degradation.

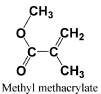
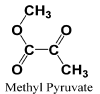
Analysis of the chromatograms obtained by GC–MS shows that the reaction product is methyl pyruvate as compared with an authentic sample, having the same retention time and fragmentation profile. We observed the ion with $m/e = 43$, characteristic of pyruvate, and also the ions with $m/e = 15$, 102, and 42 as corresponding to the fragmentation of methyl pyruvate.

According to the products observed, the main fate of the 1,2-hydroxyalkoxy radicals formed seems to be C₁–C₂ scission. This is in agreement with previous FTIR product studies on the reaction of OH with methyl methacrylate in the presence of NO_x, performed by Blanco et al.^{4,10}

Quantification of methyl pyruvate was performed by GC–FID using SPME technique for preconcentration of analytes. Table 1 shows the formation yield obtained by least-squares analysis of the data. We prefer to quote the final yield as an average of three experiments performed under the same initial conditions. At least seven chromatograms were collected during the course of each experiment. The errors quoted are 2σ statistical errors from the linear regression analysis.

The concentration–time profiles of the formation of methyl pyruvate (Figure 2) show that this is a primary product. Least-square analysis of the plot of the concentration of methyl pyruvate as a function of the amount of reacted methyl

Table 1. Formation Yields of the Oxidation Products Identified from the OH Radical Oxidation of Methyl Methacrylate in the Absence of NO_x

Compound	Product	Yield (%)	Comparison with previous determination
		(73 ± 9)%	
		(72 ± 8)%	(92 ± 16)% ^a
		(83 ± 5)%	NO _x presence
		Average	
		(76 ± 13)% ^b	
		NO _x absence	

^aBlanco et al.¹⁰ ^bThis work.

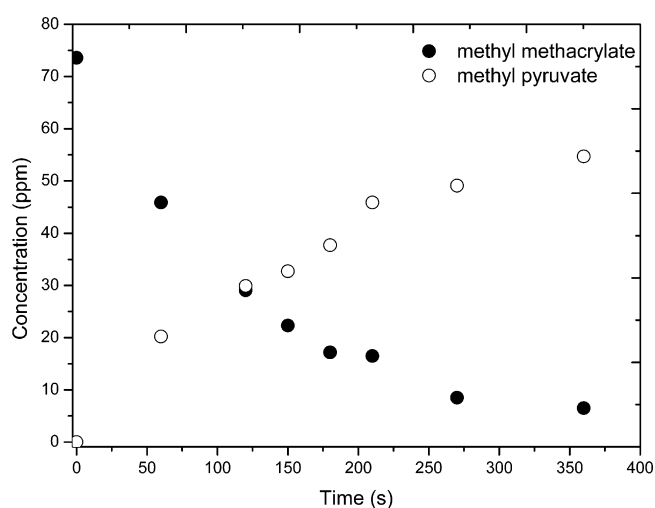


Figure 2. Plot of the concentration–time profile of methyl methacrylate and the reaction product methyl pyruvate, obtained from the sequential irradiation of the reaction mixture at NO_x-free air.

methacrylate (Figure 3) gives a molar yield of 76 ± 13%. It is expected that the contribution of secondary reactions between methyl pyruvate and OH radicals should be negligible; for that reason no corrections were made.

As suggested by Blanco et al.,¹⁰ the product branching ratios for the reactions of OH radicals with acrylate esters are particularly NO_x-sensitive; for that reason, they recommend further investigation to correctly represent the oxidation mechanisms of this class of compounds in atmospheric chemical transport (CT) models, in different scenarios (polluted and remote areas). In Table 1 the yields of the degradation channel leading to formation of methyl pyruvate show a slight variation in the presence (92%) and absence (76%) of NO_x. This leads to the assumption that the presence of NO_x could affect the reaction intermediates by promoting the molecular channels as a reaction with oxygen or isomerization. This may be due to the fact that 1,2-hydroperoxy radical intermediates after reaction with NO_x are more favored energetically, leading, preferably, to decomposition of the adduct by its instability.

Through the GC–MS technique employed in this work we could not successfully determine the presence of other organic compounds, although the contribution of other reaction channels is expected. In the absence of NO_x the peroxy radicals

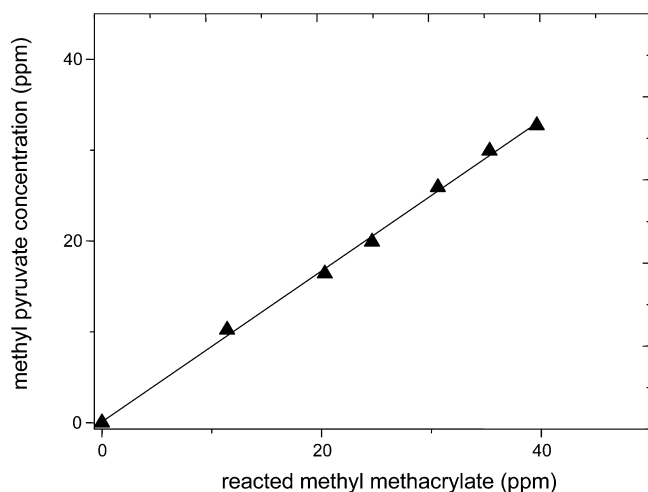


Figure 3. Plot of the concentration of the reaction product methyl pyruvate as a function of reacted methyl methacrylate obtained from irradiation of the reaction mixture methyl methacrylate–H₂O₂–air.

could undergo self- and cross-peroxy reactions which could also result, to a large extent, in the formation of 1,2-hydroxyalkoxy radicals.²⁵ Furthermore, it is known that RO₂ + RO₂/HO₂ reactions can affect the yield of the decomposition channel by the formation of hydroperoxides.²⁶ In our experimental conditions, the remaining ≈25% can be attributed to reactions between different peroxides that can lead to the formation of hydroperoxydes and organic peroxides.

6. THEORETICAL CALCULATIONS

It is well established that the initial addition and subsequent chemistry will result in the formation of 1,2-hydroxyalkoxy radical. Taking into account the degradation products observed, this work does not address other possible reactions of the OH radical toward MMA (such as hydrogen abstraction). Hence, the analysis is focused on the possible C–C fragmentations routes of RO• (channels A, B, and C of Figure 1).

Figure 4 shows possible addition channels, their associated thermochemistry, and the SOMO orbital for these processes. As can be seen, the terminal addition provides a stable conjugated adduct, whereas the alternative one generates an isolated radical whose formation is less favored. The experimental product

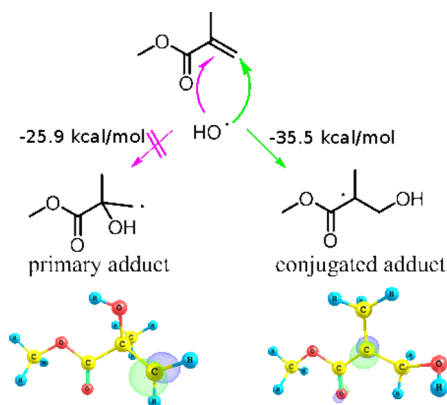


Figure 4. Schematic graph for two possible addition steps for OH radical toward methyl methacrylate (MMA) and the associated thermochemistry. The orbital SOMO is shown for resulting adducts after addition of OH radical to the double bond.

distribution shows that the initial addition occurs at the terminal olefin carbon, in agreement with the theoretically predicted stability of the two possible adducts (labeled as primary and conjugated adducts in Figure 4) due to the incoming conjugation of the most stable product, and the fact that the primary carbon is less sterically hindered than the tertiary one for the addition process. Considering that adduct progress to RO•, the possible decomposition and isomerization channels (channels A, B, C, and D in Figure 1) were simulated. A conformational analysis was performed and the most stable conformer was considered in our analysis. Reaction channels for the most stable structure of the RO• radical are represented schematically in Figure 5. Channel A

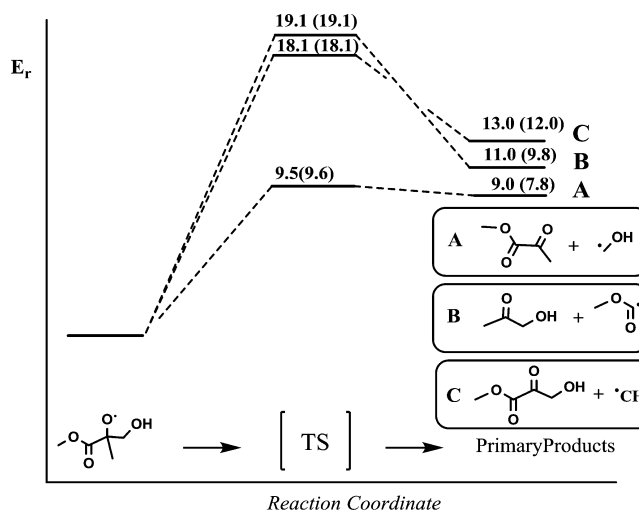


Figure 5. Schematic energy profiles for reaction channels A–C at MPWB1K/6-31+G(d,p) level. The values in parentheses are ZPE-corrected total energies at MPWB1K/6-31++G(d,p) level. Relative energies (kcal) are plotted with respect to the ground-state energy of hydroxyalkoxy radical arbitrarily taken as zero.

(C₁–C₂ scission) has the lowest energy barrier (AE = 9.5 kcal mol⁻¹), making it the most favorable reaction path. This barrier height value is in agreement with previous studies where the activation barrier was reported to be around 10 kcal mol⁻¹ for related β-hydroxyalkoxy radicals.^{27,28} On the contrary, C₂–C₃ fragmentation providing hydroxy methyl pyruvate and methyl radical ejection (channel B) shows an activation barrier of 18.1 kcal mol⁻¹. Finally, C₂–C₅ fragmentation to produce hydroxy acetone is the kinetically less favored one (AE = 19.1 kcal mol⁻¹). In addition to the kinetic data, calculations show that channel A is also the most favorable one from a thermodynamic perspective (9.0 kcal < 11.0 kcal < 13.0 kcal).

For other reaction pathways of RO• as the isomerization (channel D, Figure 1), the molecule requires two consecutive endothermic activation steps, an initial dihedral rotation to form a second conformer that later reacts through a six-membered transition state to form the corresponding alkyl radical eq 3. The dihedral rotation shows an activation energy (AE) of 8.5 kcal and the 1,5 H-shift is 7.1 kcal. The numbers between parentheses are relative energies taking the most stable conformer as reference. Thus, the isomerization is not favored compared with the case of channel A.

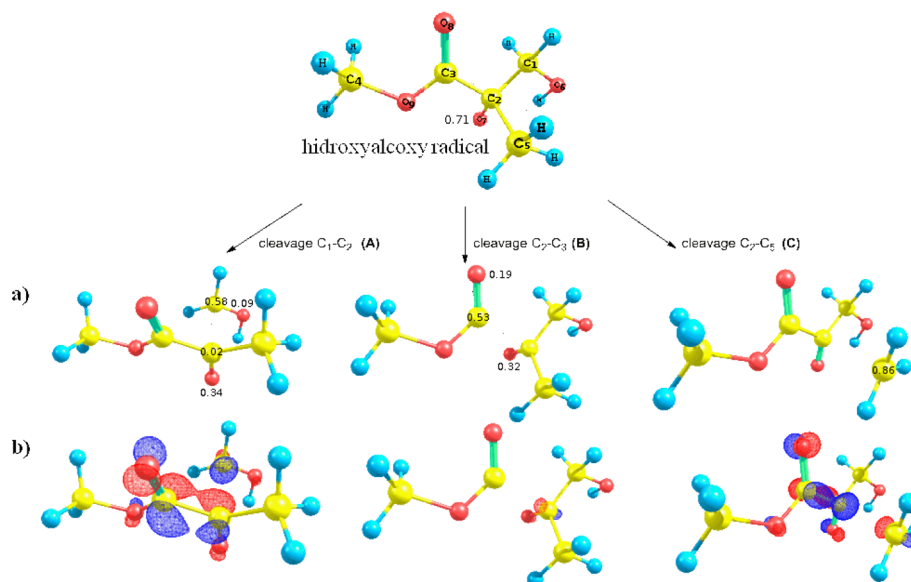
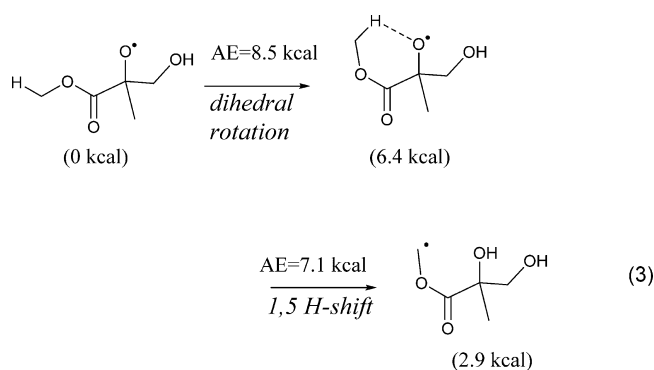


Figure 6. Transition-state structures for the fragmentation channel from hydroxyalkoxy radical (A, B, and C). (a) Main atomic spin densities obtained from Mulliken population analysis corresponding to transition-state structures. (b) Plot of molecular orbital (SOMO - 1) at the transition-state geometry.



According to these energy profiles, the reactivity of RO^\bullet with a predominance of channel A is expected given the large difference in the activation barriers calculated. In all reaction channels it was possible to characterize the corresponding transition-state structures. Figure 6 shows the optimized molecules and some relevant geometrical and electronic parameters obtained for the initial hydroxyalkoxy radical and subsequent transition states for decomposition channels. The different decomposition channels generate two fragments, one radical and its closed-shell counterpart. Both fragments require some electronic stabilization to understand the differences between the activation barriers observed. Visualization of the optimized structure of TS_A at the electronic level reveals the molecular spin density delocalized between different atoms. This effect helps to stabilize this open-shell structure. It can also be observed that, although C_1 has only part of the total spin density, the rest is localized on the oxygen atoms (O_7), favoring its stabilization by delocalization. The optimized geometry of TS_A has the four atoms (O_7 , C_2 , C_3 , and O_8), almost on the same plane. This geometry promotes a conjugation between both carbonyl groups, as shown in the molecular orbital SOMO^{-1} .

The transition state of channel C is not stabilized due to the fact that the spin density is almost entirely on the carbon of the methyl group (C_5), with high electron localization. Although the carbonyl groups also achieve conjugation (Figure 6b), the

absence of spin delocalization on the TS_C structure explains its higher energy as compared to that of TS_A .

In the latter (TS_B), an unusual electron delocalization is observed in which the carbonyl group shares the radical nature between carbon (C_3) and oxygen (O_8). Additionally, this nonplanar structure loses the conjugation between carbonyl groups, resulting in a high energy cost. The last effect allows us to understand the reason why this transition state is energetically less accessible.

In summary, TS_A has two stabilizing effects, the delocalization of the unpaired electron and π system conjugation. These two effects decrease the activation barrier for this channel, showing large differences in the alternative fragmentation path (channels B and C). These calculations can justify the formation of methyl pyruvate as the main product due to the significant difference between calculated activation energies.

Once the electronic properties that explain the oxidation of MMA are described, it is interesting to compare the product yield formed under different experimental conditions. The differences in the yields observed with and without NO_x can be analyzed by the thermodynamic differences in the associated reactions that produce 1,2-hydroxyalkoxy radicals. The Figure 7 summarizes the main thermodynamic differences found in alternative reaction channels in the presence or absence of NO_x .

In the presence of NO_x the RO^\bullet formed by the reaction between RO_2^\bullet and NO is exothermic ($-14.5 \text{ kcal mol}^{-1}$). This calculated value is within the range ($11\text{--}17 \text{ kcal mol}^{-1}$) determined for unsubstituted alkyl peroxy radicals and certain halogenated alkyl peroxy radicals.^{29–31} According to this energy profile, RO^\bullet will have considerable internal excitation energy and rapid decomposition of these activated alkoxy radicals through $\text{C}_1\text{--C}_2$ bond scission can compete effectively with collisional thermalization of the RO^\bullet radicals.

In the absence of NO_x , two possible mechanisms for the formation of RO^\bullet were considered, peroxy radical self-reaction and reaction between peroxy and OH radicals. The calculation shows that peroxy radical self-reactions are predicted to be strongly endothermic ($+33.7 \text{ kcal mol}^{-1}$), and this does not seem

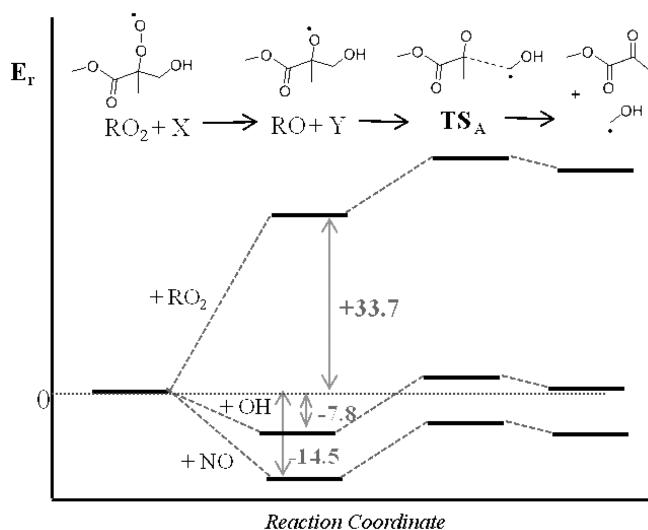
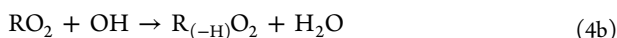
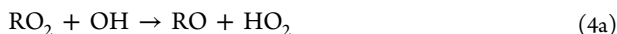


Figure 7. Schematic energy profiles for 1,2-hydroxyalkoxy radical formation and C_1 – C_2 bond fragmentation at MPWB1K/6-31+G(d,p) level. The values are ZPE-corrected total energies at the same level. Relative energies (kcal) are plotted with respect to the ground-state energy of peroxy radical taken as zero for comparative purposes.

to be a favored channel. By contrast, the peroxy radical could react with OH radical to form RO^\bullet and HO_2 by a slightly exothermic reaction path ($-7.8 \text{ kcal mol}^{-1}$) and is expected to be the dominating reaction pathway. In addition to our thermodynamic assumption, the importance of this title reaction has been demonstrated kinetically for the reaction between CH_3O_2 radical and OH radicals with a rate coefficient of $(2.8 \pm 1.4) \times 10^{-10} \text{ cm}^3 \text{ molecule}^{-1} \text{ s}^{-1}$, which is faster in comparison with the previously reported rate constant for peroxy radical self-reaction obtained by Atkinson ($(3.5 \pm 0.12) \times 10^{-13} \text{ cm}^3 \text{ molecule}^{-1} \text{ s}^{-1}$).^{15,32} Considering the high OH concentration expected under these experimental conditions and its rate coefficient, the reaction between RO_2 radical and OH radicals appears to be the fate reaction.

The title reaction may proceed via three alternative reaction paths as shown in the following equations:



It is interesting to note that the side reactions of RO_2^\bullet with OH (reactions 4b and 4c) are negligible, for MMA-derived peroxy radical. The absence of α -H in the RO_2^\bullet molecule precludes hydrogen-abstraction reaction 4b and the steric hindrance hinders S_N2 -type reaction 4c. In agreement with the product observed, only the oxygen atom transfer reaction 4a takes place and could be responsible for the yield reported.

Considering both RO^\bullet formation and the subsequent decomposition channel (channel A), which is to a thermoneutral process ($+1.2 \text{ kcal mol}^{-1}$), the RO^\bullet produced has little or no internal excitation. As a consequence, part of this intermediate could be thermalized and the reaction yield lower than that in the reaction with NO_x , as previously seen in other VOCs.³³ Evidence of these chemical activation effects in the atmospheric chemistry of different alkoxy radicals has been reported previously.^{34–36}

Although it is well-known that OH radical concentration in the atmosphere is estimated to be 100 times lower than $[RO_2^\bullet]$,

recent experimental studies demonstrated that the rate coefficient for the reaction $RO_2^\bullet + OH$ radicals ($R = CH_3$) proved to be 3 orders of magnitude higher than those determined for peroxy radical self-reaction.¹² The same study, using data from a field campaign and an atmospheric model showed that reaction between $CH_3O_2^\bullet + OH$ represents around 25% of the overall sink for $CH_3O_2^\bullet$, making this reaction as important as the reaction commonly accepted with HO_2 radicals and RO_2^\bullet .

Even though the $RO_2^\bullet + OH$ reaction in polluted atmospheres would become negligible by the presence of NO_x reaction with OH radicals in remote areas could compete with peroxy radical self-reaction. Further studies need to be considered by including other peroxy radicals (with larger alkyl chains R and with different functional groups) to clearly establish the contribution of reactions 4a–c). In the case of MMA, the present work proposes that the fate of the RO_2^\bullet formed could be the reaction with OH radicals and therefore will not be a negligible reaction channel in an atmosphere with low NO_x concentration.

In summary, product quantification under NO_x -free air and atmospheric conditions was performed. Results showed a slight variation in the presence (92%)⁸ and absence (76%) of NO_x . DFT calculations showed that the formation of methyl pyruvate is the most favorable channel. Depending on the reaction mechanism (presence or absence of NO_x) the product yield could be explained on the basis of system energy taking into account the thermochemistry associated with RO^\bullet formation.

7. CONCLUSIONS

A theoretical and experimental study was performed to understand the reaction mechanism and to determine the reaction pathway and product yields of the OH-initiated degradation of MMA in remote atmospheres.

In the absence of NO_x , methyl pyruvate was determined for the first time with a yield of $76 \pm 13\%$ according to the decomposition of the 1,2-hydroxyalkoxy radicals formed. A tendency for the reactivity of MMA was observed if the reaction occurs in the presence or absence of NO_x . For this system the effect of NO_x is lower than that observed for other VOCs.

Theoretical analysis provides insight into the prevalence of fragmentation A (C_1 – C_2 scission) at electronic level, suggesting that the formation of methyl pyruvate is kinetically and thermodynamically more favorable than that of alternative channels.

On the contrary, according to our results it is possible to explain the difference in the yield of methyl pyruvate observed in the presence or absence of NO_x . In NO_x -free conditions, the reaction between RO_2^\bullet and OH radical is expected to be slightly exothermic and to be the dominating reaction pathway in the formation of RO^\bullet because the most commonly accepted peroxy radical self-reactions proved to be strongly endothermic. In NO_x -rich environments, the reaction $RO_2^\bullet + NO$ is calculated to be even more exothermic, expressed as a higher product yield due to a chemical activation effect.

Based on the present study and previous reports, a discussion about the influence of the title reaction becomes necessary especially in NO_x -free conditions. A combined experimental and theoretical approach will be required, especially for the study of other complex peroxy radicals to fully understand the chemical reactivity and atmospheric implications of these species.

■ ASSOCIATED CONTENT

■ Supporting Information

The Supporting Information is available free of charge on the ACS Publications website at DOI: 10.1021/acs.jpca.5b04273.

Cartesian coordinates for relevant species and computational analysis of the reaction coordinates for MMA with or without NO_x including calculated energy profiles and thermochemistry (PDF)

■ AUTHOR INFORMATION

Corresponding Author

*M. A. Teruel. Fax: +54 351 4334188. E-mail address: mteruel@fcq.unc.edu.ar.

Notes

The authors declare no competing financial interest.

■ ACKNOWLEDGMENTS

The authors wish to acknowledge FONCYT, CONICET, and SeCyT-UNC for financial support. R.G.G. wishes to acknowledge doctoral fellowship and support from CONICET.

■ REFERENCES

- U.S. Environmental Protection Agency. Health and Environmental Effects Profile for Methyl Methacrylate. EPA/600/x-85/364. Environmental Criteria and Assessment Office, Office of Health and Environmental Assessment, Office of Research and Development, Cincinnati, OH, 1985.
- Kikuchi, Y.; Hirao, M.; Ookubo, T.; Sasaki, A. Design of Recycling System for Poly(Methyl Methacrylate) (PMMA). Part 2: Process Hazards and Material Flow Analysis. *Int. J. Life Cycle Assess.* **2014**, *19*, 307–319.
- Finlayson-Pitts, B. J.; Pitts, Jr. J. N. *Chemistry of the Upper and Lower Atmosphere*; Academic Press: New York, 2000.
- Blanco, M. B.; Taccone, R. A.; Lane, S. I.; Teruel, M. A. On the OH-initiated Degradation of Methacrylates in the Troposphere: Gas-Phase Kinetics and Formation of Pyruvates. *Chem. Phys. Lett.* **2006**, *429*, 389–394.
- Blanco, M. B.; Bejan, I.; Barnes, I.; Wiesen, P.; Teruel, M. A. Temperature-Dependent Rate Coefficients for the Reactions of Cl Atoms with Methyl Methacrylate, Methyl Acrylate and Butyl Methacrylate at Atmospheric Pressure. *Atmos. Environ.* **2009**, *43*, 5996–6002.
- Teruel, M. A.; Lane, S. I.; Mellouki, A.; Solignac, G.; Le Bras, G. OH Reaction Rate Constants and UV Absorption Cross-Sections of Unsaturated Esters. *Atmos. Environ.* **2006**, *40*, 3764–3772.
- Saunders, S. M.; Baulch, D. L.; Cooke, K. M.; Pilling, M. J.; Smurthwaite, P. I. Kinetics and Mechanisms of the Reactions of OH with some Oxygenated Compounds of Importance in Tropospheric Chemistry. *Int. J. Chem. Kinet.* **1994**, *26*, 113–130.
- Lawler, M. J.; Finley, B. D.; Keene, W. C.; Pszenny, A. A. P.; Read, K. A.; von Glasow, R.; Saltzman, E. S. Pollution-enhanced Reactive Chlorine Chemistry in the Eastern Tropical Atlantic Boundary Layer. *Geophys. Res. Lett.* **2009**, *36*, L08810.
- Spicer, C. W.; Chapman, E. G.; Finlayson-Pitts, B. J.; Plastring, R. A.; Hubbe, J. M.; Fast, J. D.; Berkowitz, C. M. Unexpectedly High Concentrations of Molecular Chlorine in Coastal Air. *Nature* **1998**, *394*, 353–356.
- Blanco, M. B.; Bejan, I.; Barnes, I.; Wiesen, P.; Teruel, M. A. Products and Mechanism of the Reactions of OH Radicals and Cl Atoms with Methyl Methacrylate (CH₂=C(CH₃)C(O)OCH₃) in the Presence of NO_x. *Environ. Sci. Technol.* **2014**, *48*, 1692–1699.
- Smith, D. F.; McIver, C. D.; Kleindienst, T. E. Primary Product Distribution from the Reaction of Hydroxyl Radicals with Toluene at ppb NO_x Mixing Ratios. *J. Atmos. Chem.* **1998**, *30*, 209–228.

(12) Onel, L.; Blitz, M.; Dryden, M.; Thonger, L.; Seakins, P. Branching Ratios in Reactions of OH Radicals with Methylamine, Dimethylamine, and Ethylamine. *Environ. Sci. Technol.* **2014**, *48*, 9935–9942.

(13) US Environmental Protection Agency, 2000. AOPWIN v1.91. Washington, D.C., <http://www.epa.gov/opptintr/exposure/docs/episuite.htm>.

(14) Fittschen, K.; Whalley, L. K.; Heard, D. E. The Reaction of CH₃O₂ Radicals with OH Radicals: A Neglected Sink for CH₃O₂ in the Remote Atmosphere. *Environ. Sci. Technol.* **2014**, *48*, 7700–7701.

(15) Bossolasco, A.; Faragó, E. P.; Schoemaëcke, C.; Fittschen, C. Rate Constant of the Reaction Between CH₃O₂ and OH Radicals. *Chem. Phys. Lett.* **2014**, *593*, 7–13.

(16) Archibald, A. T.; Petit, A. S.; Percival, C. J.; Harvey, J. N.; Shallcross, D. E. On the Importance of the Reaction Between OH and RO₂ Radicals. *Atmos. Sci. Lett.* **2009**, *10*, 102–108.

(17) Gao, R.; Zhu, L.; Zhang, Q.; Wang, W. Atmospheric Oxidation Mechanism and Kinetic Studies for OH and NO₃ Radical-Initiated Reaction of Methyl Methacrylate. *Int. J. Mol. Sci.* **2014**, *15*, 5032–5044.

(18) Frisch, M. J.; Trucks, G. W.; Schlegel, H. B.; Scuseria, G. E.; Robb, M. A.; Cheeseman, J. R.; Scalmani, G.; Barone, V.; Mennucci, B.; Petersson, G. A.; et al. *Gaussian 09*, Revision B.01; Gaussian, Inc.: Wallingford, CT, 2010.

(19) Zhao, Y.; Truhlar, D. G. Hybrid Meta Density Functional Theory Methods for Thermochemistry, Thermochemical Kinetics, and Non-covalent Interactions: The MPWB1B95 and MPWB1K Models and Comparative Assessments for Hydrogen Bonding and van der Waals Interactions. *J. Phys. Chem. A* **2004**, *108*, 6908–6918.

(20) Mishra, B. K. Theoretical Investigation on the Atmospheric Fate of the CF₃C(O)OCH(O)CF₃ radical: alpha-ester rearrangement vs. oxidation. *RSC Adv.* **2014**, *4*, 16759–16764.

(21) Mishra, B. K.; Lily, M.; Deka, R. C.; Chandra, A. K. Theoretical Investigation on Gas-Phase Reaction of CF₃CH₂OCH₃ with OH Radicals and Fate of Alkoxy Radicals (CF₃CH(O)OCH₃/CF₃CH₂OCH₂O). *J. Mol. Graphics Modell.* **2014**, *50*, 90–99.

(22) Deka, R. C.; Mishra, B. K. A Theoretical Investigation on the Kinetics, Mechanism and Thermochemistry of Gas-Phase Reactions of Methyl Acetate with Chlorine Atoms at 298 K. *Chem. Phys. Lett.* **2014**, *595*, 43–47.

(23) Gonzalez, C.; Schlegel, H. B. An Improved Algorithm for Reaction Path Following. *J. Chem. Phys.* **1989**, *90*, 2154–2161.

(24) Hratchian, H. P.; Schlegel, H. B. Using Hessian Updating to Increase the Efficiency of a Hessian Based Predictor-Corrector Reaction Path Following Method. *J. Chem. Theory Comput.* **2005**, *1*, 61–69.

(25) Lightfoot, P. D.; Cox, R. A.; Crowley, J. N.; Destriau, M.; Hayman, G. D.; Jenkin, M. E.; Moortgat, G. K.; Zabel, F. Organic Peroxy Radicals: Kinetics, Spectroscopy and Tropospheric Chemistry. *Atmos. Environ., Part A* **1992**, *26A*, 1805–1964.

(26) Navarro, M. A.; Dusanter, S.; Hites, R. A.; Stevens, P. S. Radical Dependence of the Yields of Methacrolein and Methyl Vinyl Ketone from the OH-Initiated Oxidation of Isoprene under NO_x-Free Conditions. *Environ. Sci. Technol.* **2011**, *45*, 923–929.

(27) Vereecken, L.; Peeters, J. Theoretical Investigation of the Role of Intramolecular Hydrogen Bonding in β-Hydroxyethoxy and β-Hydroxyethylperoxy Radicals in the Tropospheric Oxidation of Ethane. *J. Phys. Chem. A* **1999**, *103*, 1768–1775.

(28) Orlando, J. J.; Tyndall, G. S.; Bilde, M.; Ferronato, C.; Wallington, T. J.; Vereecken, L.; Peeters, J. Laboratory and Theoretical Study of the Oxy Radicals in the OH- and Cl-Initiated Oxidation of Ethene. *J. Phys. Chem. A* **1998**, *102*, 8116–8123.

(29) Atkinson, R.; Baulch, D. L.; Cox, R. A.; Hampson, R. F., Jr; Kerr, J. A.; Rossi, M. J.; Troe, J. Evaluated Kinetic and Photochemical Data for Atmospheric Chemistry, Organic Species: Supplement VII. *J. Phys. Chem. Ref. Data* **1999**, *28*, 191–393.

(30) Schneider, W. F.; Nance, B. I.; Wallington, T. J. Bond Strength Trends in Halogenated Methanols: Evidence for Negative Hyperconjugation? *J. Am. Chem. Soc.* **1995**, *117*, 478–485.

(31) Schneider, W. F.; Wallington, T. J.; Barker, J. R.; Stahlberg, E. A. $\text{CF}_3\text{CFHO}^\bullet$ Radical: Decomposition vs. Reaction with O_2 . *Ber. Bunsen-Ges* **1998**, *102*, 1850–1856.

(32) Atkinson, R.; Baulch, D. L.; Cox, R. A.; Crowley, J. N.; Hampson, R. F.; Hynes, R. G.; Jenkin, M. E.; Rossi, M. J.; Troe, J. Evaluated Kinetic and Photochemical Data for Atmospheric Chemistry: Volume II—Gas Phase Reactions of Organic Species. *Atmos. Chem. Phys.* **2006**, *6*, 3625–4055.

(33) Blanco, M. B.; Bejan, I.; Barnes, I.; Wiesen, P.; Teruel, M. A. Atmospheric Oxidation of Vinyl and Allyl Acetate: Product Distribution and Mechanisms of the OH-Initiated Degradation in the Presence and Absence of NO_x . *Environ. Sci. Technol.* **2012**, *46*, 8817–8825.

(34) Hurley, M. D.; Wallington, T. J.; Bjarrum, M.; Javadi, M. S.; Nielsen, O. J. Atmospheric Chemistry of 3-Pentanol: Kinetics, Mechanisms, and Products of Cl Atom and OH Radical Initiated Oxidation in the Presence and Absence of NO_x . *J. Phys. Chem. A* **2008**, *112*, 8053–8060.

(35) Hurley, M. D.; Wallington, T. J.; Laursen, L.; Javadi, M. S.; Nielsen, O. J.; Yamanaka, T.; Kawasaki, M. Atmospheric Chemistry of n-Butanol: Kinetics, Mechanisms, and Products of Cl Atom and OH Radical Initiated Oxidation in the Presence and Absence of NO_x . *J. Phys. Chem. A* **2009**, *113*, 7011–7020.

(36) Thüner, L. P.; Barnes, I.; Becker, K. H.; Wallington, T. J.; Christensen, L. K.; Orlando, J. J.; Ramacher, B. Atmospheric Chemistry of Tetrachloroethene ($\text{Cl}_2\text{C CCl}_2$): Products of Chlorine Atom Initiated Oxidation. *J. Phys. Chem. A* **1999**, *103*, 8657–8663.